Eur. Phys. J. B **59**, 47–54 (2007)
DOI: 10.1140/epjb/e2007-00258-4

THE EUROPEAN PHYSICAL JOURNAL B

Analytic study of electron transmission through serial mesoscopic metallic rings

W.Y. Cui, S.Z. Wu, G. Jin[a], X. Zhao[b], and Y.Q. Ma

National Laboratory of Solid State Microstructures and Department of Physics, Nanjing University, Nanjing 210093, P.R. China

Received 8 February 2006 / Received in final form 1st September 2007
Published online 5 October 2007 – © EDP Sciences, Società Italiana di Fisica, Springer-Verlag 2007

Abstract. We investigate the electron transmission through a structure of serial mesoscopic metallic rings coupled to two external leads. A set of analytical expressions based on the quantum waveguide transport and the transfer matrix method are derived and used to discuss the effects of geometric configurations on transmission probabilities. It is found that in the contact ring case the existence of an applied magnetic flux is necessary to create transmission gaps, while in the non-contact ring case transmission gaps always appear irrespective of whether there is an applied magnetic flux or not. The transmissions for periodic rings with a defect ring and periodic rings built by two sorts of rings are also briefly studied. It is also found that the transmission periodicity with wave vector must be ensured by the commensurability of two characteristic lengths, i.e., of the half perimeter of a ring and the connecting wire between two adjacent rings. The special points of wave vector and magnetic flux which give rise to the transmission resonance and antiresonance are analyzed in detail.

PACS. 73.23.Ad Ballistic transport – 73.63.Nm Quantum wires – 73.21.Hb Quantum wires – 85.35.Be Quantum well devices

1 Introduction

In the past two decades, considerable attention has been paid to the propagation of electron waves along quantum wires with various geometric structures [1–27]. Among these quantum confined structures, the mesoscopic metallic rings are the most attractive. It has been made clear that the geometry of rings is significant for electron transport, especially that the magnetic flux threading rings can change the phases of wave functions, leading to constructive or destructive interferences and bringing about the periodic oscillations in transmission amplitudes. There are two important effects in these Aharonov-Bohm (AB) rings. One is the band formation [1,3,7,8], and the other is the persistent current [1,4,6,15]. Both are due to the existence of magnetic flux through the rings. Besides, the notion of AB cages becomes prominent in recent years and it states that an extreme localization mechanism can be induced by magnetic fields in some quantum networks made of one-dimensional wires [13,17,20]. Recent experimental progress in creating quantum coherent devices in metallic as well as in semiconductor nanostructures indicates the principal ability to perform magnetotransport based on serial connecting rings [18,19]. So far the quantum transport in mesoscopic rings has been an exciting research field, but the behavior in serially connected ring systems has not been sufficiently explored analytically.

In the present work we perform an analytic study of the transport in the ideal mesoscopic metallic rings connected one after another by perfect metallic wires, which can be realized experimentally by modern micro-fabrication technologies. Similar structures have been studied by using the free-electron model [8] and the tight-binding model [11,24], respectively. To deal with the problems efficiently and analytically, we use the method of quantum waveguide transport on networks as well as the powerful transfer-matrix approach which has been proved to be reliable [5,10,22,23]. For simplicity, we assume that an electron moves ballistically through the serial rings and wires, and scatterings can only take place at the junctions between two rings or a ring and a wire. Simple as it is, this model can capture the essential features of the quantum coherence occurring in quasi-one-dimensional metallic periodic rings, which could be realized in single-channel clean metallic rings. It may be noted that if disorder is introduced, such as there exist impurities in the quantum

[a] e-mail: gjin@nju.edu.cn
[b] *Permanent address*: Zhejiang Institute of Modern Physics, Zhejiang University, Hangzhou 310027, P.R. China.

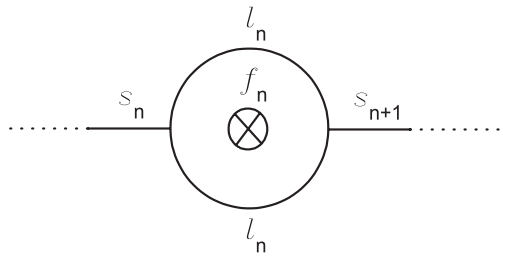

Fig. 1. A segment of a serial mesoscopic metallic ring structure.

wires, the electron motion will be diffusive at low temperatures. This case of diffusive transport will be involved in the elastic scatterings in multi-channels and is out of the scope of the present paper.

The paper is organized as follows: Section 2 is devoted to the model and formulation for investigating the electron transmission through a serial metallic ring structure. In Section 3 the numerical results and discussions are presented for the dependence of electron transmission on the magnetic flux and electronic wave vector in the cases for various geometrical parameters. Finally, a summary is given in Secton 4.

2 Model and formulation

We consider a one-dimensional serial ring structure composed of N rings and $N+1$ wires. Wires 1 and $N+1$ are the leads connected to the two ends of an external reservoir, while wire n connects the $(n-1)$th ring and the nth ring. One segment of this structure is shown in Figure 1 with the coordinate x along the waveguide. The wave functions describing the incoming wave and the transmitted wave on the two sides of the serial ring structure are taken to be plane-wave like, i.e., $\psi_1 = e^{ikx} + re^{-ikx}$ with r denoting the reflection amplitude, and $\psi_{N+1} = te^{ikx}$ with t denoting the transmission amplitude. Similarly, the wave functions in the nth wire, the upper arm and lower arm of the nth ring can be written as $\psi_n = A_n e^{ikx} + B_n e^{-ikx}$, $\psi_n^{(u)} = C_n e^{ikx} + D_n e^{-ikx}$ and $\psi_n^{(l)} = E_n e^{ikx} + F_n e^{-ikx}$ if there is no magnetic field.

When a magnetic field exists, the one-dimensional Sch-rödinger equation for a single ring is

$$\left[\frac{1}{2m}\left(\frac{\hbar}{i}\frac{d}{dx} + \frac{e}{c}\frac{\phi}{l}\right)^2 + V(x)\right]\psi(x) = E\psi(x), \quad (1)$$

where ϕ is the magnetic flux through the ring. For the present case, no tunnel potential barrier is assumed to exist in the system, namely, $V(x) = 0$. Therefore, the wave function $\psi(x)$ is still a superposition of plane waves with the wave vector k. We can choose a gauge for the vector potential $\mathbf{A}$ in which the effect of the magnetic field appears as a change in the phase of wave functions. Thus the wave functions for an electrons in the upper and lower arms of a ring moving in the clockwise and anti-clockwise directions are

$$\psi^{(u)} = (Ce^{ikx} + De^{-ikx})e^{\frac{ie\phi}{\hbar cl}x}, \quad (2)$$

and

$$\psi^{(l)} = (Ee^{ikx} + Fe^{-ikx})e^{-\frac{ie\phi}{\hbar cl}x}. \quad (3)$$

It should be stressed that a local coordinate is chosen for each ring with its origin being located at the left intersection. In this prescription, all accumulated phases from previous rings and wires are included in the coefficients in equations (2) and (3). When an electron travels along the upper (lower) arm of the ring, it acquires a phase factor $e^{i\pi f}$ $(e^{-i\pi f})$ with f being the reduced magnetic flux

$$f = \frac{e\phi}{hc} = \frac{e}{hc}\oint_{\mathbf{l}} \mathbf{A}\cdot d\mathbf{l}, \quad (4)$$

where $hc/e = \phi_0$ is the magnetic flux quantum, $\mathbf{l}$ is along the ring and l is the half perimeter (each ring is assumed to be symmetrically divided by two wires). To establish the relations of the coefficients in the plane-wave representation, we would invoke the Griffith's boundary conditions which ensure the continuity of wave functions and the conservation of current density at the intersections [5,14]. It is worthy of pointing out that this kind of boundary conditions is consistent with the scattering matrix method with the coupling $\epsilon = 4/9$ in reference [4] as well as with the parameters $m = 3$, $w = 1$ and $\lambda = 0$ in reference [21] in which the author gave a generalization of the scattering theory onto arbitrary graphs made of one-dimensional wires connected to external leads.

By applying the boundary conditions at the two intersections of the nth ring, the electronic wave amplitudes in the $(n+1)$th wire can be obtained from the amplitudes in the nth wire,

$$\begin{pmatrix} A_{n+1} \\ B_{n+1} \end{pmatrix} = T_{n+1,n}\begin{pmatrix} A_n \\ B_n \end{pmatrix}, \quad (5)$$

where $T_{n+1,n}$ is a 2×2 transfer matrix. Since the length of the connecting wire s_n and the half perimeter of the ring l_n are combined with the wave vector k, we take l_n, s_n and k to be all dimensionless quantities. By a transformation

$$\begin{pmatrix} A_n \\ B_n \end{pmatrix} = \begin{pmatrix} 1 & i \\ 1 & -i \end{pmatrix}\begin{pmatrix} \alpha_n \\ \beta_n \end{pmatrix}, \quad (6)$$

$T_{n+1,n}$ is transformed into $M_{n+1,n}$ for a new set of amplitudes (α_n, β_n), which satisfies

$$\begin{pmatrix} \alpha_{n+1} \\ \beta_{n+1} \end{pmatrix} = M_{n+1,n}\begin{pmatrix} \alpha_n \\ \beta_n \end{pmatrix}, \quad (7)$$

where

$$M_{n+1,n} = \begin{pmatrix} \dfrac{\cos(kl_n)}{\cos(\pi f_n)} & -\dfrac{\sin(kl_n)}{2\cos(\pi f_n)} \\ \dfrac{2\cos^2(\pi f_n) - 2\cos^2(kl_n)}{\sin(kl_n)\cos(\pi f_n)} & \dfrac{\cos(kl_n)}{\cos(\pi f_n)} \end{pmatrix} \times \begin{pmatrix} \cos(ks_n) & -\sin(ks_n) \\ \sin(ks_n) & \cos(ks_n) \end{pmatrix}. \quad (8)$$

Then the complex transfer matrix, $T_{n+1,n}$, is transformed into the real one, $M_{n+1,n}$, which gives great convenience for the following analytic calculation. With these transfer matrices, we have

$$\begin{pmatrix} \alpha_{N+1} \\ \beta_{N+1} \end{pmatrix} = M(N) \begin{pmatrix} \alpha_1 \\ \beta_1 \end{pmatrix}, \tag{9}$$

where

$$M(N) = \prod_{n=1}^{N} M_{n+1,n} \tag{10}$$

is the global transfer matrix of the whole system. After the matrix $M(N)$ was obtained, the electronic transport through the system can be determined by the transmission coefficient

$$T = \frac{4}{2 + |M(N)|^2}, \tag{11}$$

where $|M(N)|^2$ is defined here as the sum of the squares of its four matrix elements. It is obvious that equations (8)–(11) are quite general formulas for any serial metallic ring structure. Choose the parameters l_n, s_n, and f_n properly, we can investigate, for example, the Fibonacci sequence of metallic rings as well [24]. After the structural parameters are given, in principle, the electronic density distribution and transmission property can be determined as a function of the magnetic flux and electronic wave vector, the latter is equivalent to the electronic energy in the free-electron model. For concreteness, in the following, we would discuss the periodic ring structure, partly due to its convenience to be realized in experiments [18,19].

In the case of periodic rings, all rings are identical, so are the transfer matrices. It is easy to write a single matrix M by replacing l_n, f_n and s_n in equation (8) with l, f and s. The total transfer matrix $M(N)$ is obtained by

$$M(N) = M^N = u_{N-1}(\chi)M - u_{N-2}(\chi)I, \tag{12}$$

where I is the unit matrix and $u_N(\chi)$ is the Chebyshev polynomial of the second order with the trace defined by $\chi = \frac{1}{2}\mathrm{Tr}M$. Combining equations (11) and (12), we get

$$T = \frac{1}{1 + C(kl, f)u_{N-1}^2(\chi)}, \tag{13}$$

where

$$C(kl, f) = \frac{[4\sin^2(\pi f) - 3\sin^2(kl)]^2}{16\sin^2(kl)\cos^2(\pi f)}, \tag{14}$$

and

$$\chi = \frac{\cos(kl)}{\cos(\pi f)}\cos(ks) + \frac{4\sin^2(\pi f) - 5\sin^2(kl)}{4\cos(\pi f)\sin(kl)}\sin(ks). \tag{15}$$

Equations (13)–(15) are the core equations in the following discussions. By changing the parameters, such as the lengths of connecting wires, the perimeter of rings, and the magnetic flux threading rings, a serial ring structure exhibits many fascinating phenomena.

Specifically, in the case of contact rings, that is $s = 0$, equation (15) is simply replaced by

$$\chi = \frac{\cos(kl)}{\cos(\pi f)}. \tag{16}$$

Combining it with equations (13) and (14), the transmission coefficient for contact rings can be calculated. As a byproduct, the precise expressions for the transmission coefficient of single-ring and double-ring structures without connecting wires can thus be derived easily. Both expressions from our approach are in perfect agreement with the former study [22].

However, in more general cases, such as for N taking any integer or even for s not zero, using our analytical results, the transmission properties can be extensively studied. For example, we can easily find the resonant transmission ($T = 1$) and antiresonant transmission ($T = 0$) conditions. When $f = m + 1/2$, for m being an integer, the phase shift between the electronic wave functions in the upper arms and lower arms is $(2m + 1)\pi$ at the intersections. This gives the zero transmission. We can also find that when $f \neq m$ and kl is an integral multiple of π, the transmission coefficient is also zero. It is interesting to find all points for the resonant transmission. From equation (13), it is clear that the resonant transmission is a combined effect of wave vector k and piercing flux f if the length l is given. Therefore, the following two conditions,

$$C(kl, f) = 0, \tag{17}$$

or

$$u_{N-1}(\chi) = 0, \tag{18}$$

can lead to the resonant transmission, respectively. Equation (17) gives a universal condition of the resonant transmission for all periodic ring structures. It reads

$$\frac{\sin^2(\pi f)}{\sin^2(kl)} = \frac{3}{4}, \tag{19}$$

which is independent of the number of identical rings N. Equation (18) renders

$$\chi = \cos(m\pi/N), m = 1, \cdots, N-1, \tag{20}$$

which, by combining with equation (15), gives different resonant transmissions in the (k, f) plane for different N.

3 Numerical results and discussions

We start our discussion with the special case where the rings contact with each other. In Figure 2, the transmission coefficient T, for a chain with 100 contact rings, is shown as a function of the reduced magnetic flux f for several values of wave vector k. If the ring radius is made to be $r = 0.1$ μm, according to $f = \phi/\phi_0 = \pi e r^2 B/hc$, the magnetic field is experimentally feasible. Since l is always combined with k, we can fix $l = 1$ here and also in all later discussions. Because T is an even and periodic

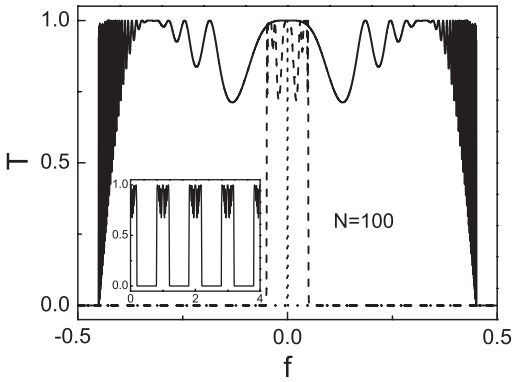

Fig. 2. Transmission coefficient T versus reduced magnetic flux f of a chain with 100 contact rings. Solid,dotted and dashed lines represent $kl = 0.45\pi$, π and 0.05π, respectively. The inset shows the transmission coefficient in a wider f range with $kl = 0.2\pi$.

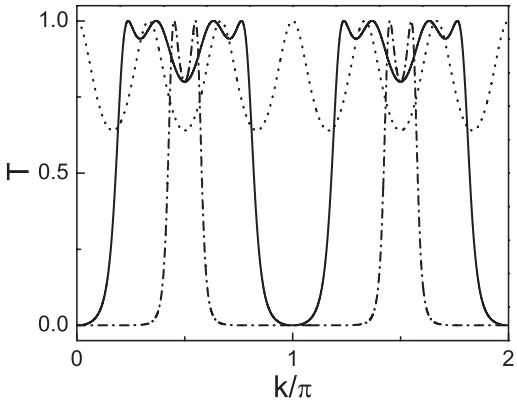

Fig. 3. Transmission coefficient T versus wave vector k for a three ring system. Dotted line, $f = 0$; solid line, $f = 1/5$; dash dotted line, $f = 2/5$.

function of f with the period 1, we show it only within one period of f, from -0.5 to 0.5. The transmission coefficient never drops to zero when $\cos(kl)/\cos(\pi f) \leq 1$ and always equals zero when $\cos(kl)/\cos(\pi f) > 1$ if the number of rings is large enough. The inset in Figure 2 gives an exhibition of the transmission coefficient versus the magnetic flux f in a little wider range. It clearly shows that the electron transmission coefficient, corresponding to the electron conductance, can be tuned by the external magnetic flux. This property gives a possibility to apply to electronic devices, for example, a magnetic switch with the turnover point at $\cos(kl) = \cos(\pi f)$.

For contact rings, another interesting phenomenon is the flux-independent total transmission. It appears only in the even-numbered ring geometry. When $kl = \pi/2$ but the magnetic flux f changes, the transmission coefficient T always equals 1 except at the half integer f points. By the way, the half integer f is an absolute condition for $T = 0$ which overrides the condition of flux-independent total transmission [22]. This can be verified from the expressions involved in the transmission coefficient. When $kl = \pi/2$ and f is not a half integer,

$$\chi = 0, \tag{21}$$

then

$$u_{N-1}(\chi) = \begin{cases} 1 \text{ or } -1, & N \text{ is odd}, \\ 0, & N \text{ is even}. \end{cases} \tag{22}$$

So in this situation the resonant transmission ($T = 1$) is always satisfied for even-numbered rings.

The transmission coefficient T versus wave vector k for the contact rings is shown in Figure 3. In the simplest case, $f = 0$, the transmission coefficient satisfies

$$T = \frac{32}{41 - 9\cos(2Nkl)}. \tag{23}$$

Resonant transmission can be obtained by requiring that $\cos(2Nkl) = 1$ and the solutions are simply given by $k = m\pi/(Nl)$ with m being any integer. There is no transmission zero at all in this case. The magnitude of the transmission minimum is a constant $T = 0.64$. However, when a perpendicular magnetic flux is applied to the contact rings, transmission zero appears. In accordance with this result is that the spin-orbit interaction, which can be controlled by a gate voltage in the Rashba mechanism, will provide an effective magnetic field to create conduction gaps in the serial contact rings [26,27].

It deserves to point out that for N contact rings, $N+1$ resonant peaks will appear, instead of only $N-1$ resonant peaks as the conventional cognition from the electron transmission through semiconductor superlattices [7]. The positions of these $N+1$ resonant peaks are strictly given by equations (17)–(20). Taking three rings for example, if the magnetic flux f is 1/5, there exist four resonant peaks of T ($k = 0.237\pi, 0.763\pi, 0.367\pi, 0.633\pi$) in one period π, as is shown by the solid line in Figure 3. The first two are caused by equation (19) and the latter two by equation (20). The dash dotted line in this figure represents the transmission coefficient versus wave vector k when $f = 2/5$, and only two peaks can be observed in one period. This is because $|\sin(2\pi/5)| > \sqrt{3}/2$ which excludes the possibility of any k value for resonant transmission due to equation (19). It is noticed that as the number of rings increases, the transmission valleys became sharper and sharper, and change into gaps. For the contact ring case,

$$|\chi| = \left|\frac{\cos(kl)}{\cos(\pi f)}\right| > 1 \tag{24}$$

is responsible for the gaps, which is very easy to verify by using equation (13) for the transmission coefficient. As $\chi > 1$, $\lim_{N\to\infty} u_{N-1}^2 \to \infty$, then $T \to 0$.

To show the wave vector and magnetic flux dependence of transmission coefficient simultaneously, we can plot a $T - k - f$ three-dimensional diagram for contact rings. However, a three-dimensional diagram cannot show the transmission properties clearly because the majority of transmission peaks are difficult to distinguish. For a better

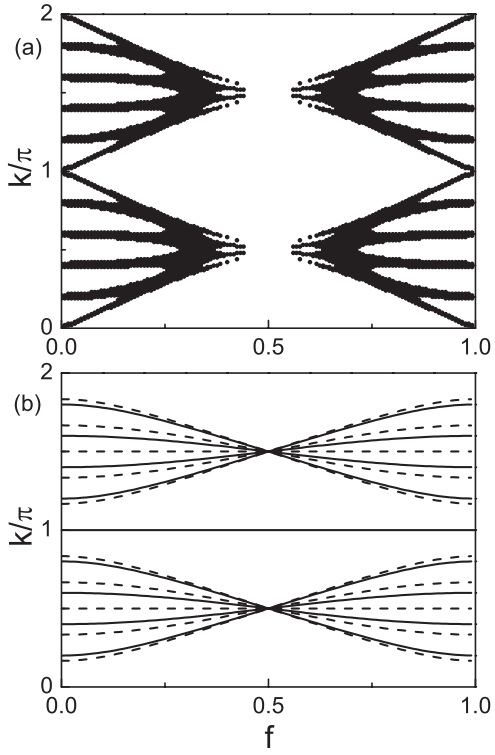

Fig. 4. Transmission spectrum and energy spectra shown in the wave vector k versus magnetic flux f plane. (a) Transmission spectrum of a five contact ring system. The dots represent the total transmission coefficient of an incident electron $T \geq 0.95$; (b) energy spectra for five (solid line) and six (dashed line) contact ring structures.

exhibition of transmission properties, we would like to plot here the points in the $k - f$ plane with a transmission coefficient no less than 0.95 in the three-dimensional diagram, as is shown in Figure 4a. This result is roughly consistent with Figure 6 in reference [11], in which the resonant transport properties were studied in the tight-binding model. The energy spectrum, also in the contact ring regime, can be given by using the fixed boundary conditions for the wave functions at both ends of the whole system. From these boundary conditions, we have

$$\frac{\sin(kl)}{\cos(\pi f)} u_{N-1}(\chi) = 0, \tag{25}$$

which implies the dispersion relation $k - f$. Comparing it with equations (17)–(20) which render transmission peaks, we can find that they are very similar. $u_{N-1}(\chi) = 0$ gives corresponding solutions not only for the transmission peaks but also for the eigenenergies. When the energy of an incident electron equals one of these $N - 1$ eigenenergies, the electron will transmit through this system ballistically. We plot the energy spectrum in Figure 4b. It is consistent with the transmission spectrum in Figure 4a. It is not difficult to elucidate that the small differences between these two figures come from different boundary conditions.

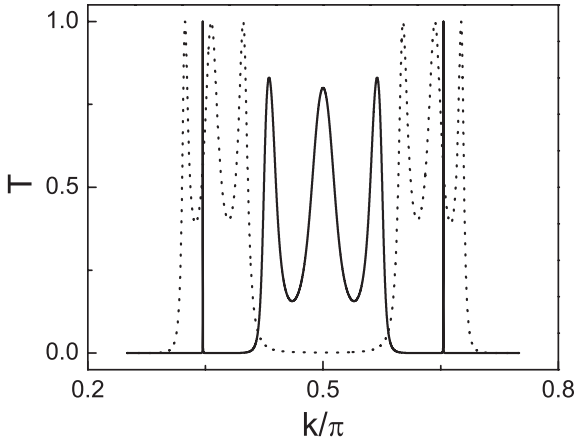

Fig. 5. Transmission coefficient T versus wave vector k for a nine ring system with a defect ring and an eight ring system built by two sorts of rings. The parameters are $f_1 = 2/5$, $f_2 = 1/5$. Solid line is for the former case and dotted line is for the latter case.

In Figure 4, as well as in Figure 2, we can find that the reduced magnetic flux $f = 1/2$ always corresponds to the zero transmission. This reminds us the theoretical prediction and experimental confirmation of the AB cages which describe the set of sites eventually visited by a wave packet that can be confined for particular values of the magnetic flux [13,17,20]. It is attributed to the AB destructive interference on a special topological structure when the flux per elementary plaquette equals half a quantum magnetic flux. It is no doubt that there are some similarities between the serial metallic rings and the bipartite tilling of rhombus for the localization due to magnetic phase interferences, although the former is much simpler than the latter.

Another interesting case we would like to show below is that of a defect ring inserted in the middle of contact rings. We can get the total transfer matrix by multiplying the transfer matrices for single rings one after another, so finally the transmission coefficient is obtained. Although defects can have other configurations, here the defect ring is assumed to have the same size of the normal rings while the piercing flux is different. The transmission coefficient T versus wave vector k for a nine ring system is shown by the solid line in Figure 5, where the fluxes in the normal rings and the defect ring are taken to be $f_1 = 2/5$ and $f_2 = 1/5$, respectively. We can observe two isolated modes $k = 0.34659\pi$ and $k = 0.65340\pi$ in addition to the transmission band. These two isolated modes are symmetric about $k = \pi/2$. We know that in the absence of any defect ring, i.e., $f_2 = f_1$, the high transmission regions forming bands correspond to $|\chi| \leq 1$ with χ defined as $\cos(kl)/\cos(\pi f)$. But when $f_2 \neq f_1$, there may exist narrow transmission bands satisfying $|\chi| > 1$. This is true not only when there are only a few rings but also when the number of rings increases. As the number of rings becomes infinite, the isolated transmission points can be obtained

analytically from

$$T_{j1}^2 + T_{j2}^2 + 2T_{j1}T_{j2}\frac{\cos(kl)}{\cos(\pi f_1)} = 0, \tag{26}$$

where

$$T_{j1} = \frac{2\cos(kl)[4\cos^2(kl) - 2\cos^2(\pi f_1) - \cos^2(\pi f_2)]}{\cos^2(\pi f_1)\cos(\pi f_2)},$$
$$T_{j2} = \frac{4\cos^2(kl) - \cos^2(\pi f_1) - \cos^2(\pi f_2)}{\cos(\pi f_1)\cos(\pi f_2)}. \tag{27}$$

As $f_1 = 2/5$ and $f_2 = 1/5$, there are two solutions very close to the case for nine rings. They are $k = 0.34658\pi$ and $k = 0.65341\pi$. Numerical calculation also confirms that the isolated bands become narrower and narrower as the ring number increases.

The transmission coefficient for a periodic ring structure built by two sorts of rings can also be analyzed. In this case the primary transfer matrix is a multiplication of the two original transfer matrices. And we can give the transmission formulas in the same manner with a Chebyshev polynomial as for identical rings. Here if the rings are of the same size while the fluxes are different, the trace is given as

$$\chi = \frac{4\cos^2(kl) - \cos^2(\pi f_1) - \cos^2(\pi f_2)}{\cos(\pi f_1)\cos(\pi f_2)}. \tag{28}$$

As was shown for the identical ring case, χ here is responsible for the transmission band. This renders that for $0 < f_2 < f_1 < \pi/2$, the transmission band satisfies

$$\frac{\cos(\pi f_2) - \cos(\pi f_1)}{2} \leq |\cos(kl)| \leq \frac{\cos(\pi f_2) + \cos(\pi f_1)}{2}. \tag{29}$$

In general, a transmission band for identical rings is separated into two subbands as is shown by the dotted line in Figure 5.

We now turn to the more general case when the rings are connected via metallic wires. The transmission coefficient becomes dependent on the length of wires. The effect of s can be seen from equation (15), the expression of the half matrix trace χ. In this case, $f = m + 1/2$ also renders the transmission zeros, because of the AB interference. The conditions responsible for the resonant transmission still arises from $C(kl, f) = 0$ or $u_{N-1}(\chi) = 0$. We plot in Figure 6 the transmission coefficient versus piercing magnetic flux f for a nine ring system. Figure 6 also shows the role of the connecting wire length s in the transmission spectrum. It is shown, by the dashed line, there are two isolated peaks in one period. $C(kl, f) = 0$ is responsible for this phenomenon. As the number of rings increases, the resonant peaks becomes sharper but the isolated peaks always exist.

We have shown that in the contact ring case, when there is no piercing flux, the transmission coefficient never approaches zero. But for serial rings with connecting wires, there exist transmission zeros in the zero-flux case. This is due to the effect of ks in equation (15), which gives a change in χ. And when χ is larger than 1, the transmission zero appears. We plot here the transmission coefficient versus wave vector for a five ring system in Figures 7a and 7b. The transmission bands are clearly separated by the band gaps. The transmission coefficient T for the non-contact rings with a magnetic flux is shown in Figures 7c and 7d, in comparison with the zero flux case. We can observe that $k = m\pi$, for m being an integer, gives the resonant transmission in the zero flux case, but the antiresonant transmission in the finite flux case.

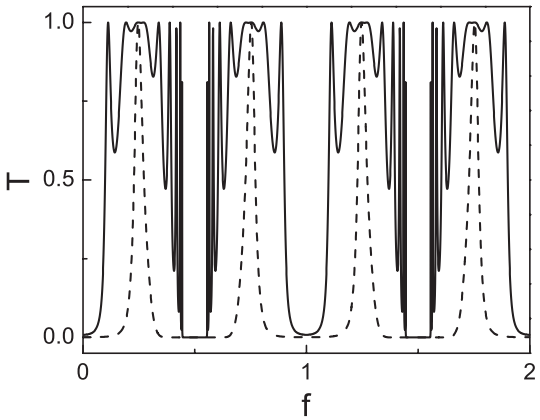

Fig. 6. Transmission coefficient T versus reduced magnetic flux f of a nine ring system for $kl = 0.3\pi$. Solid line, $s = 1.7$; dashed line, $s = 2.6$.

Since the rings are connected via wires in the non-contact case, it is clear that the periodicity and symmetry of the transmission spectra are closely related to the relative ratio of s and l. There are two distinct cases: the commensurate case when the ratio is a rational number and the incommensurate case when the ratio is an irrational number. Since l is fixed at 1 throughout this paper, the length s can be taken to represent the relative ratio. For the commensurate case, the periodicity and the symmetry of the transmission spectra always exist, which can be seen from Figures 7a and 7c when $s = 0.5$. The period and the resonant transmission points can also be determined from the expression for the transmission coefficient. For the incommensurate case, we cannot find any periodicity and symmetry for the transmission spectra, or to say, the period is infinite, as is shown in Figures 7b and 7d for which we take $s = (\sqrt{5} - 1)/2$, the reciprocal of the well-known golden mean.

4 Summary

We have theoretically studied the electron transmission through structures of periodically arranged mesoscopic metallic rings. The rings can be coupled by either direct contact or connecting wires, and they can be threaded with or without magnetic flux. In the ballistic regime and considering scattering at the junctions, a set of analytic expressions have therefore been derived and have effectively been used to discuss various situations. By our formulation, it is easy to determine the resonant and antiresonant transmissions for any multi-ring structure, for

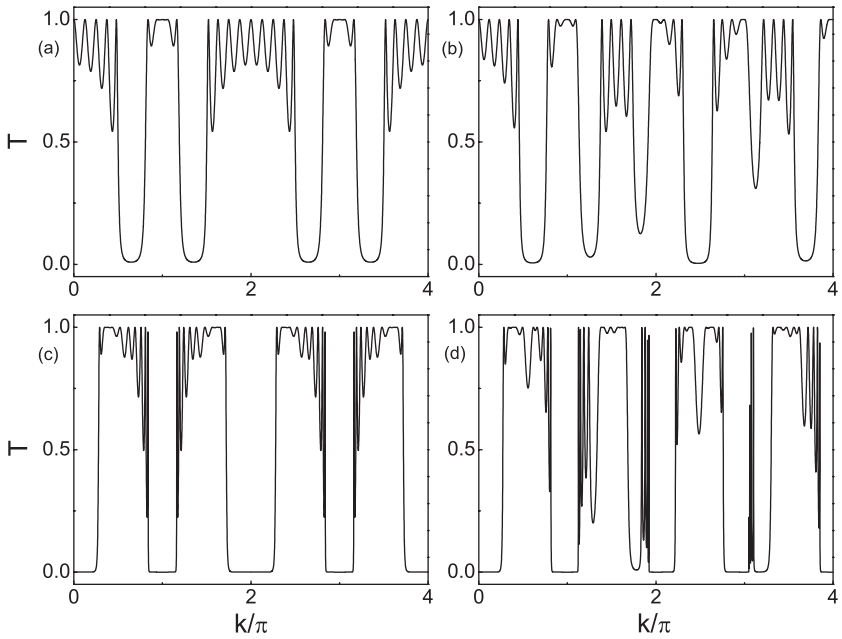

Fig. 7. Transmission coefficient T versus wave vector k of a five ring system. (a) $f = 0$, $s = 0.5$; (b) $f = 0$, $s = (\sqrt{5}-1)/2$; (c) $f = 0.3$, $s = 0.5$; (d) $f = 0.3$, $s = (\sqrt{5}-1)/2$.

example, there are the absolute transmission zeros at the half-integer quantum magnetic flux threading rings. It has been found that for the contact ring structure a magnetic flux is necessary to cause transmission gaps. It has been demonstrated that the number of resonant transmission peaks for a N-ring structure in a period of wave vector is generally $N+1$, instead of $N-1$ in the case of semiconductor superlattices. The flux-independent total transmission has also been analytically investigated. Furthermore, the role of connecting wire length in transmission spectra was studied. Our results have shown that the nonzero length of connecting wires can provide another approach to produce transmission gaps even without introducing any magnetic flux. We have pointed out the importance of commensurability between the lengths of the half perimeter of a ring and connecting wire of neighboring two rings. The wave vector dependence of transmission spectra can be periodic in the commensurate case or aperiodic in the incommensurate case, even though the serial ring structure is kept periodic. The transmission for periodic rings with a defect ring and periodic rings built by two sorts of rings are also briefly addressed and isolated modes and band separation are found.

Due to the great advance now in the growth and fabrication of nanostructures, it is not difficult to create a line of connected rings up to several tens or even hundreds [18,19]. It should be noted that these experiments were performed in the diffusive cases, since the considered rings gave the conducting channels of the order of several tens or even more than thousands. It is expected that the one-channel ballistic transport in serial mesoscopic rings can be realized in experiments one day after the further progress in micro-manufacture. Ultralow temperature can be used to insure the phase coherence [16]. The interesting results in this work suggest to experimentally verify the controllable output of electrons by varying the magnetic flux threading the rings. By the way, it is also meaningful for the transmission with selectivity of electronic wave vectors. It should be emphasized that although our results are presented in perfect one-dimensional rings, they can still be valid for real rings with finite width, provided that the width of rings is comparable to the characteristic Fermi wave length of a system. Based on the fascinating features stated above, it could be expected that this kind of serial ring structures may have potential applications in the next generation of electronic devices.

This work was supported by the Natural Science Foundation 10674058 and 60371013, and the State Key Program 2006CB921803 of China.

References

1. M. Büttiker, Y. Imry, R. Landauer, Phys. Lett. A **96** , 365 (1983)
2. Y. Gefen, Y. Imry, M.Y. Azbel, Phys. Rev. Lett. **52**, 129 (1984)
3. R. Landauer, M. Büttiker, Phys. Rev. Lett. **54**, 2049 (1985)
4. M. Büttiker, Phys. Rev. B **32**, R1846 (1985)
5. J.B. Xia, Phys. Rev. B **45**, 3593 (1992)
6. P.A. Mello, Phys. Rev. B **47**, 16358 (1993)
7. D. Takai, K. Ohta, Phys. Rev. B **50**, 2685 (1994)
8. P. Singha Deo, A.M. Jayannavar, Phys. Rev. B **50**, 11629 (1994)
9. A.M. Jayannavar, P. Singha Deo, Phys. Rev. B **51** 10175 (1995)

10. J.R. Shi, B.Y. Gu, Phys. Rev. B **55**, 4703 (1997)
11. J.B. Li, Z.Q. Zhang, Y.Y. Liu, Phys. Rev. B **55**, 5337 (1997)
12. G.J. Jin, Z.D. Wang, A. Hu, S.S. Jiang, Phys. Rev. B **55**, 9302 (1997)
13. J. Vidal, R. Mosseri, B. Douçot, Phys. Rev. Lett. **81**, 5888 (1998)
14. G.J. Jin, Z.D. Wang, A. Hu, S.S. Jiang, J. Appl. Phys. **85**, 1597 (1999)
15. M. Pascaud, G. Montambaux, Phys. Rev. Lett. **82**, 4512 (1999)
16. A.B. Gougam, F. Pierre, H. Pothier, D. Esteve, N.O. Birge, J. Low Temp. Phys. **118**, 447 (2000)
17. J. Vidal, G. Montambaux, B. Douçot, Phys. Rev. B **62**, R16294 (2000)
18. E.M.Q. Jariwala, P. Mohanty, M.B. Ketchen, R.A. Webb, Phys. Rev. Lett. **86**, 1594 (2001)
19. W. Rabaud, L. Saminadayar, D. Mailly, K. Hasselbach, A. Benoît, B. Etienne, Phys. Rev. Lett. **86**, 3124 (2001)
20. C. Naud, G. Faini, D. Mailly, Phys. Rev. Lett. **86**, 5104 (2001)
21. C. Texier, G. Montambaux, J. Phys. A: Math. Gen. **34**, 10307 (2001)
22. J. Yi, J.H. Wei, J. Hong, S.I. Lee, Phys. Rev. B **65**, 033305 (2001)
23. M. Moskalets, M. Büttiker, Phys. Rev. B **68**, 161311 (2003)
24. A. Chakrabarti, R.A. Römer, M. Schreiber, Phys. Rev. B **68**, 195417 (2003)
25. W. Park, J. Hong, Phys. Rev. B **69**, 035319 (2004)
26. B. Molnár, P. Vasilopoulos, F.M. Peeters, Appl. Phys. Lett. **85**, 612 (2004)
27. D. Bercioux, M. Governale, V. Cataudela, V.M. Ramaglia, Phys. Rev. Lett. **93**, 056802 (2004)